



The rectifier and inverter are using three-level Neutral Point Clamped (NPC) converter with VSC converters

M Srinu¹, Shaik Dawood²

¹M.Tech(PS) Nimra Institute of Science and Technology, Vijayawada, AP

²Asst Professor Dept of EEE, Nimra Institute of Science and Technology, Vijayawada, AP

Abstract

In this paper forced-commutated Voltage-Sourced Converter (VSC) interconnection is used to transmit power from a 230 kV, 2000 MVA, 50 Hz system to another identical AC system. The rectifier and the inverter are three-level Neutral Point Clamped (NPC) VSC converters using close IGBT/Diodes. The Sinusoidal Pulse Width Modulation (SPWM) switching uses a single-phase triangular carrier wave with a frequency of fundamental frequency. Along with the converters, the station includes on the AC side, the step down Yg-D transformer, the AC filters, the converter reactor and on the DC side the capacitors, the DC filters. The discrete control system generates the three sinusoidal modulating signals that are the reference value of the bridge phase voltages. The amplitude and phase of the modulating signals can be calculated to control either: the reactive and real AC power flow at the PCC, or the reactive power flow at the PCC and the pole to pole DC voltage.

I. INTRODUCTION

DUE to the world energy crisis and environmental problems caused by conventional power generation, renewable energy sources such as photovoltaic (PV) and wind generation

systems are becoming more promising alternatives to replace conventional generation units for electricity generation [1], [2]. Advanced power electronic systems are needed to utilize and develop renewable energy sources. In solar PV or wind energy applications, utilizing maximum power from the source is one of the most important functions of the power electronic systems. In three-phase applications, two types of power electronic configurations are commonly used to transfer power from the renewable energy resource to the grid: single-stage and double-stage conversion. In the double-stage conversion for a PV system, the first stage is usually a dc/dc converter and the second stage is a dc/ac inverter. The function of the dc/dc converter is to facilitate the maximum power point tracking (MPPT) of the PV array and to produce the appropriate dc voltage for the dc/ac inverter. The function of the inverter is to generate three-phase sinusoidal voltages or currents to transfer the power to the grid in a grid-connected solar PV system or to the load in a stand-alone system [3] [5]. In the single-stage connection, only one converter is needed to fulfill the double-stage functions, and hence the system will have a lower cost and higher efficiency, however, a more complex control method will be required. The current norm of the industry for high power applications is a three-phase, single-stage PV energy systems by using a voltage-source converter (VSC) for power conversion [4].

II. STRUCTURE OF A THREE-LEVEL INVERTER AND ITS CAPACITOR VOLTAGE CONSIDERATIONS

A. Three-Level Inverter

Since the introduction of three-level inverters in 1981 [6],[7], they have been widely used in several applications, such

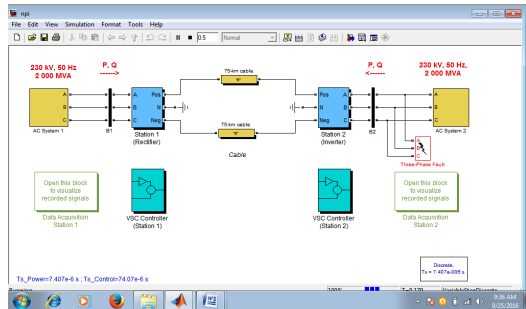


Fig 1:Typical three-level inverter (a) structure of circuit,

as: motor drives, STATCOM, HVDC, pulsewidth modulation (PWM) rectifiers, active power filters (APFs), and renewable energy applications [7], [8]. Fig. 1(a) shows a typical three phase three-level neutral-point-clamped (NPC) inverter circuit topology. The converter has two capacitors in the dc side to produce the three-level ac-side phase voltages. Normally, the capacitor voltages are assumed to be balanced, since it has been reported that unbalance capacitor voltages can affect the acside voltages and can produce unexpected behavior on system parameters such as even-harmonic injection and power ripple [7], [9]. Several papers have discussed methods of balancing these capacitor voltages in various applications [6], [7], [2] [4].

B. Balanced Capacitors Voltage

Various strategies have been proposed to balance the capacitor voltages using modulation algorithms such as sinusoidal carrier based PWM (SPWM) or space vector pulse width modulation (SVPWM) [7]. In SPWM applications, most of the strategies are based on injecting the appropriate zero-sequence signal into the modulation signals to balance the dc-link capacitors [2], [3], [6], [8].

In SVPWM applications, a better understanding of the effects of the switching options on the capacitor voltages in the vector space has resulted in many strategies proposed to balance capacitors voltages in the three-level NPC inverter. These include capacitor balancing using conventional SVPWM, virtual SVPWM (VSVPWM) and their combination [4], [5], [9]. In vector control theory, ideally, the inverter must be able to generate the voltage output instantaneously, following the reference vector (\underline{V}_{ref}), generated by the control system. However, because of the limitation of the switches in the inverter, it is not possible to guarantee that any requested vector can be generated; as a matter of fact, only a limited number of vectors (27 vectors for three-level inverter) can be generated. To overcome such difficulties, in any space vector modulation (SVM) scheme such as SVPWM and VSVPWM, the reference vector \underline{V}_{ref} is generated by selecting the appropriate available vectors in each time frame in such a way that the average of the applied vectors must be equal to the reference vector.

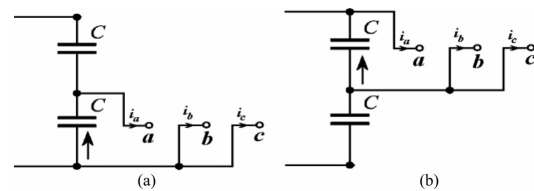


Fig. 2. Equivalent circuit and capacitors current with two different short vector.

Equation (1) shows the mathematical relation between the timing of the applied vectors and the reference vector

$$\begin{cases} T_s \vec{V}_{\text{ref}} = \sum_{i=1}^n T_i \vec{V}_i \\ T_s = \sum_{i=1}^n T_i \end{cases} \quad (1)$$

where T_s is the time frame and preferred to be as short as possible. It can be considered as a control update period where an average vector will be mathematically generated during this time duration. T_i is the corresponding time segment for selected inverter vector \vec{V}_i and n is the number of applied vectors. Generally, the reference vector is generated by three different vector ($n = 3$), and (1) can be converted to three different equation with three variables T_1 , T_2 , and T_3 to be calculated. Several vector PWM techniques presented in [6], [7], [9] [10], and [3] [5] apply similar technique of timing calculation. Fig. 1(b) shows the space vector diagram of a three-level inverter for balanced dc-link capacitors [6]. It is made up of 27 switching states, from which 19 different voltage vectors can be selected. The number associated with each vector in Fig. 1(b) represents the switching state of the inverter phases respectively. Capacitor balancing in most reported three-level NPC inverter applications is achieved by the proper selection of the short vectors.

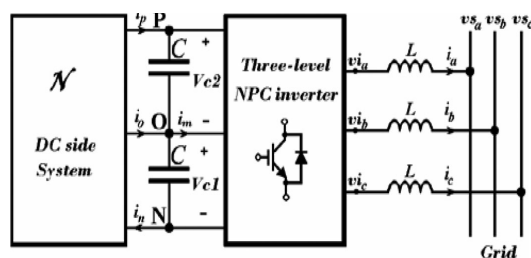


Fig. 3. General diagram of a grid connected three-wire three-level inverter.

In order to produce the ac-side waveform, the vector diagram of Fig. 1(b) is used, where the dc capacitor voltages are assumed to be balanced. Fig. 1(b) can then be used to determine the appropriate vectors to be selected and to calculate their corresponding timing (T_i) for implementing the required reference vector based on the expression given in (1). Although the control system is trying to ensure balanced capacitor voltages, should any unbalance occur during a transient or an unexpected operation, the above method will produce an inaccurate ac-side waveform which can be different from the actual requested vector by the control system. This can result in the production of even-harmonics, unbalanced current and unpredicted dynamic behavior.

C. Unbalanced Capacitor Voltages

Fig. 3 shows a general structure of a grid-connected three-level inverter showing the dc and ac sides of the inverter. The dc-side system, shown as N can be made up of many circuit configurations, depending on the application of the inverter. For instance, the dc-side system can be a solar PV, a wind generator with a rectifying circuit, a battery storage system or a combination of these systems where the dc voltage across each capacitor can be different or equal. One of the main ideas of this paper is to have an overall view of the switching effects on a three-wire connection of a three-level NPC inverter with a combination of these systems on the dc side. Mathematically, in a three-wire connection of a two-level inverter, the $dq0$ field, v_d , v_q , and v_0 of the inverter in vector control can be considered as having two degrees of freedom in the control system; because the zero sequence voltage, v_0 will have no effect on the system behavior in both the dc and the ac side of the inverter. However, in the three-level three-wire application illustrated in Fig. 3,

with fixed v_d and v_q although v_0 will have no effect on the ac-side behavior, it can be useful to take advantage of v_0 to provide a new degree of freedom to control the sharing of the capacitor voltages in the dc bus of the inverter. By doing this, it is now possible to operate and control the

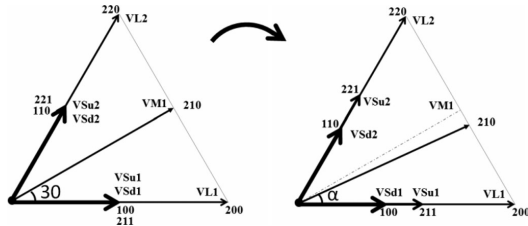


Fig 4: Vector diagram in the first sector of Fig. 1(b) showing the change of the vectors using balanced dc and unbalanced dc assuming $V_{c1} < V_{c2}$.

inverter under both balanced and unbalanced capacitor voltages while continuing to generate the correct voltages in the ac side. This feature is particularly useful in applications where the two capacitor voltages can be different, such as when connecting two PV modules with different MPPT points, or connecting a PV module across the two capacitors and including battery storage at the midpoint of the two capacitors, or connecting battery storage to each of the capacitors with the ability to transfer different power from each battery.

III. SIMULATION AND VALIDATION OF THE PROPOSED TOPOLOGY AND CONTROL SYSTEM

Simulations have been carried out using MATLAB/Simulink to verify the effectiveness of the proposed topology and control system. An *LCL* filter is used to connect the inverter to the grid. Fig. 5 shows the block diagram of the simulated system.

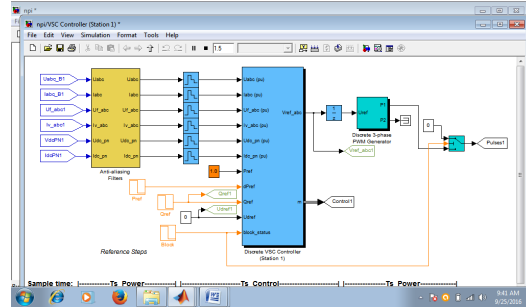


Fig. 5. Block diagram of the simulated system.

As discussed in Section III-B, G_2 must be much more than G_1 in order to achieve the MPPT condition and to have the flexibility to charge and discharge of the battery. Based on our experiments, any value more than 100 is suitable for this ratio. On the other hand, because the ratio of G_2 / G_1 will only affect the short-vector selection, increasing this ratio will not affect other results. This value has been selected to be 200 to have good control on V_{dc} , as shown in Table I. The role of *LBAT* is to smooth the battery current, especially in the transient condition. A wide range of values are acceptable for the inductor value, however, decreasing its value will increase the current overshoot of the battery. Also, its value is dependent of its adjacent capacitor value and its transient voltages. Due to the practical considerations (such as size and cost), the value of *LBAT* is preferred to be low and has been chosen to be 5 mH based our simulation studies. The values of K_p and K_i are selected by modeling the system in the *dq*-frame. The current control loop can be converted to a simple system after using the decoupling technique shown in Fig 7. The details of this method can be found in [1]. For theoretical purposes, two different scenarios have been simulated to investigate the effectiveness of the proposed topology.

A. First Scenario

In the first scenario, it is assumed that the solar irradiation will produce $I_{SC} = 5.61$ A

in the PV module according to (21). The MPPT control block, shown in Fig. 7, determines the requested PV module voltage V_{dc} , which is 117.3 V to achieve the maximum power from the PV system that can generate 558 W of electrical power. The requested active power to be transmitted to the grid is initially set at 662 W and is changed to 445 W at time $t = 40$ ms and the reactive power changes from zero to 250 VAR at time $t = 100$ ms. Fig. 9 shows the results of the first scenario simulation. Fig. 9(a) and (b) shows that the proposed control system has correctly followed the requested active and reactive power, and Fig. 9(c) shows that the PV voltage has been controlled accurately (to be 177.3 V) to obtain the maximum power from the PV module. Fig. 9(d) shows that battery is discharging when the grid power is more than the PV power, and it is charging when the PV power is more than the grid power. Fig. 9(d) shows that before time $t = 40$ ms, the battery discharges at 1.8 A since the power generated by the PV is insufficient. After time $t = 40$ ms, the battery current is about 1.8 A, signifying that the battery is being charged from the extra power of the PV module. Fig. 9(e) shows the inverter ac-side currents, and Fig. 9(f) shows the grid-side currents with a THD less than 1.29% due to the LCL filter. The simulation results in Fig. 9 show that the whole system produces a very good dynamic response. Fig. 10 shows the inverter waveforms for the same scenario. Fig. 10(a) shows the line-to-line voltage V_{ab} , and Fig. 10(b) shows the phase to midpoint voltage of the inverter V_{ao} . Fig. 10(c) and (e) shows V_{ao} , V_{on} , and V_{an} after mathematical filtering to determine the average value of the PWM waveform.

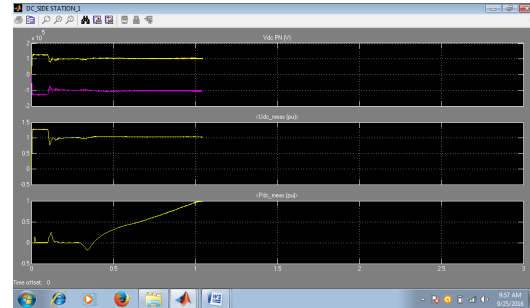


FIG A

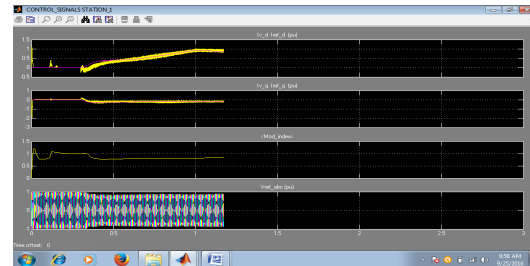


FIG B

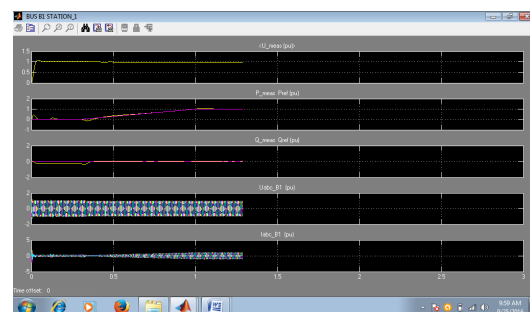


FIG C

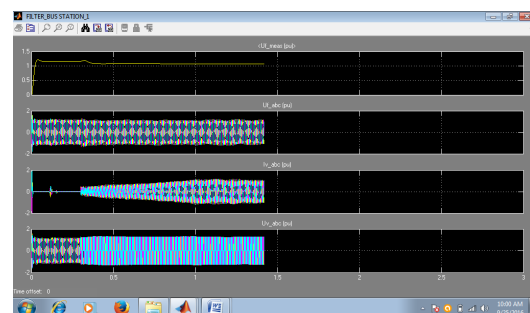


FIG D

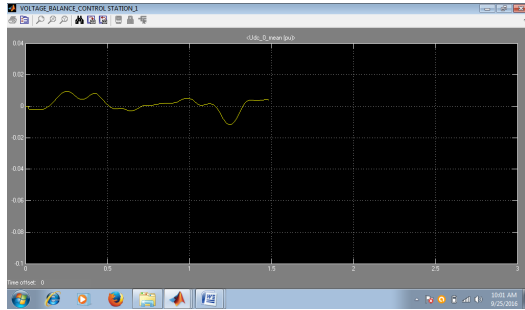


FIG E

FIG 6A,B,C,D,E :simulation at first station

B. Second Scenario

In the second scenario, it is assumed that the solar irradiation will change such that the PV module will produce $I_{SC} = 4.8, 4,$ and 5.61 A. The MPPT control block determines that V_{dc} needs to be 115.6, 114.1, and 117.3 V to achieve the maximum power from the PV units which can generate 485, 404, and 558 W, respectively. The requested active power to be transmitted to the grid is set at a constant 480 W and the reactive power is set to zero during the simulation time.

Fig. 11 shows the results of the second scenario simulation. Fig. 11(a) shows that the inverter is able to generate the requested active power. Fig. 11(b) shows that the PV voltage was controlled accurately for different solar irradiation values to obtain the relevant maximum power from the PV modules. Fig. 11(c) shows that the charging and discharging of the battery are correctly performed. The battery has supplemented the PV power generation to meet the requested demand by the grid. Fig. 11(d) illustrates that the quality of the waveforms of the grid-side currents are acceptable, which signifies that the correct PWM vectors are generated by the proposed control strategy. By using the proposed strategy, the inverter is able to provide a fast transient response. Fig. 11(e) shows the a -phase voltage

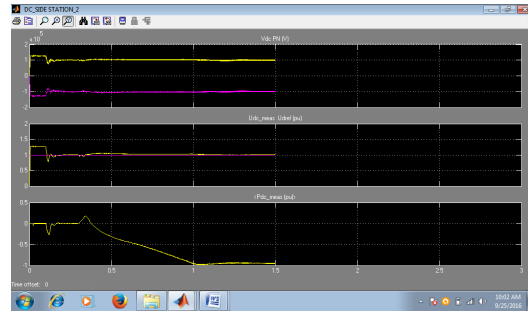


FIG A

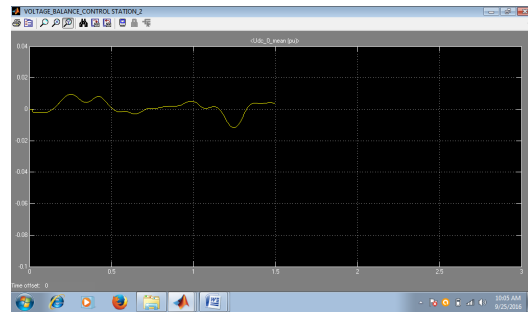


FIG B

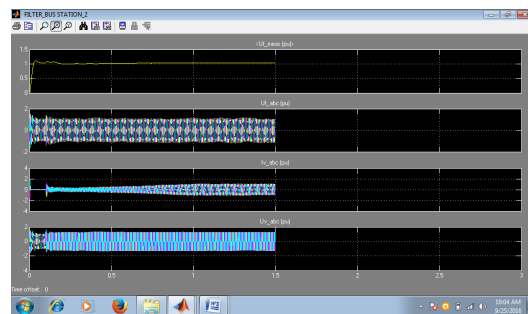


FIG C

FIG 7A,B,C:simulation outputs at station 2

IV. CONCLUSION

A novel topology for a three-level NPC voltage source inverter that can integrate both renewable energy and battery storage on the dc side of the inverter has been presented. A theoretical framework of a novel extended unbalance three-level vector modulation technique that can generate the correct ac voltage under unbalanced dc voltage conditions has been proposed. A new control algorithm for the proposed system has also been presented in order to control power flow between



solar PV, battery, and grid system, while MPPT operation for the solar PV is achieved simultaneously. The effectiveness of the proposed topology and control algorithm was tested using simulations and results are presented. The results demonstrate that the proposed system is able to control ac-side current, and battery charging and discharging currents at different levels of solar irradiation. The results from experiments using a prototype built in the lab have validated the proposed topology to control both PV and battery storage in supplying power to the ac grid.

REFERENCES

- [1] O. M. Toledo, D. O. Filho, and A. S. A. C. Diniz, Distributed photovoltaic generation and energy storage systems: A review, *Renewable Sustainable Energy Rev.*, vol. 14, no. 1, pp. 506–511, 2010.
- [2] M. Bragard, N. Soltan, S. Thomas, and R. W. De Doncker, The balance of renewable sources and user demands in grids: Power electronics for modular battery energy storage systems, *IEEE Trans. Power Electron.*, vol. 25, no. 12, pp. 3049–3056, Dec. 2010.
- [3] A. Yazdani and P. P. Dash, A control methodology and characterization of dynamics for a photovoltaic (PV) system interfaced with a distribution network, *IEEE Trans. Power Del.*, vol. 24, no. 3, pp. 1538–1551, Jul 2009.
- [4] A. Yazdani, A. R. Di Fazio, H. Ghoddami, M. Russo, M. Kazerani, J. Jatskevich, K. Strunz, S. Leva, and J. A. Martinez, Modeling guidelines and a benchmark for power system simulation studies of three-phase single-stage photovoltaic systems, *IEEE Trans. Power Del.*, vol. 26, no. 2, pp. 1247–1264, Apr. 2011.
- [5] M. A. Abdullah, A. H. M. Yatim, C. W. Tan, and R. Saidur, A review of maximum power point tracking algorithms for wind energy systems, *Renewable Sustainable Energy Rev.*, vol. 16, no. 5, pp. 3220–3227, Jun. 2012.
- [6] S. Burusteta, J. Pou, S. Ceballos, I. Marino, and J. A. Alzola, Capacitor voltage balance limits in a multilevel-converter-based energy storage system, in *Proc. 14th Eur. Conf. Power Electron. Appl.*, Aug./Sep. 2011, pp. 1–9.
- [7] L. Xinchun, Shan Gao, J. Li, H. Lei, and Y. Kang, A new control strategy to balance neutral-point voltage in three-level NPC inverter, in *Proc. IEEE 8th Int. Conf. Power Electron. ECCE Asia*, May/Jun. 2011.
- [8] J. Rodriguez, S. Bernet, P. K. Steimer, and I. E. Lizama, A survey on neutral-point-clamped inverters, *IEEE Trans. Ind. Electron.*, vol. 57, no. 7, pp. 2219–2230, Jul. 2010.
- [9] A. Lewicki, Z. Krzeminski, and H. Abu-Rub, Space-vector pulsewidth modulation for three-level npc converter with the neutral point voltage control, *IEEE Trans. Ind. Electron.*, vol. 58, no. 11, pp. 5076–5086, Nov. 2011.
- [10] J. Pou, D. Boroyevich, and R. Pindado, Effects of imbalances and nonlinear loads on the voltage balance of a neutral-point-clamped inverter, *IEEE Trans. Power Electron.*, vol. 20, no. 1, pp. 123–131, Jan. 2005.